# Physical tuning of galectin-3 signaling

Shaheen A. Farhadi[a], Renjie Liu[a], Matthew W. Becker[a], Edward A. Phelps[a], and Gregory A. Hudalla[a,1]

[a]J. Crayton Pruitt Family Department of Biomedical Engineering, University of Florida, Gainesville, FL 32611

Edited by Barbara Imperiali, Massachusetts Institute of Technology, Cambridge, MA, and approved April 6, 2021 (received for review November 20, 2020)

**Galectin-3 (Gal3) exhibits dynamic oligomerization and promiscuous binding, which can lead to concomitant activation of synergistic, antagonistic, or noncooperative signaling pathways that alter cell behavior. Conferring signaling pathway selectivity through mutations in the Gal3–glycan binding interface is challenged by the abundance of common carbohydrate types found on many membrane glycoproteins. Here, employing alpha-helical coiled-coils as scaffolds to create synthetic Gal3 constructs with defined valency, we demonstrate that oligomerization can physically regulate extracellular signaling activity of Gal3. Constructs with 2 to 6 Gal3 subunits ("Dimer," "Trimer," "Tetramer," "Pentamer," "Hexamer") demonstrated glycan-binding properties and cell death–inducing potency that scaled with valency. Dimer was the minimum functional valency. Unlike wild-type Gal3, which signals apoptosis and mediates agglutination, synthetic Gal3 constructs induced cell death without agglutination. In the presence of CD45, Hexamer was distributed on the cell membrane, whereas it clustered in absence of CD45 via membrane glycans other than those found on CD7. Wild-type Gal3, Pentamer, and Hexamer required CD45 and CD7 to signal apoptosis, and the involvement of caspases in apoptogenic signaling was increased in absence of CD45. However, wild-type Gal3 depended on caspases to signal apoptosis to a greater extent than Hexamer, which had greater caspase dependence than Pentamer. Diminished caspase activation downstream of Hexamer signaling led to decreased pannexin-1 hemichannel opening and interleukin-2 secretion, events facilitated by the increased caspase activation downstream of wild-type Gal3 signaling. Thus, synthetic fixation of Gal3 multivalency can impart physical control of its outside-in signaling activity by governing membrane glycoprotein engagement and, in turn, intracellular pathway activation.**

signal transduction | galectin-3 | emergent function | multivalency | coiled-coil

Proteins exhibit an extraordinarily diverse range of functions, including catalyzing biochemical reactions, regulating ion flux, machining gene replication, and activating signaling cascades. A recent shift in this paradigm shows that certain proteins demonstrate emergent functions upon dynamic assembly of individual subunits (1, 2). Multivalent interactions enabled by this dynamic assembly orchestrate complex events within living systems; however, while multivalency is a functional determinant of high affinity binding, it is also operatively linked to fluctuating promiscuity (3). For instance, signaling of dimeric vascular endothelial growth factor (VEGF) in tumor cells is regulated through differences in relative affinities for cognate receptors VEGFR1 and VEGFR2, coupled with secretion of the soluble form of VEGFR1 that functions as a decoy receptor to diminish VEGFR2 signaling (4). Tumor necrosis factor–related apoptosis-inducing ligand (TRAIL), a homotrimeric protein known for its exceptional selectivity and apoptotic signaling activity toward cancer cells, exhibits decreased death receptor (e.g., DR4 and DR5) signaling sensitivity in the presence of inhibitory decoy death receptors (e.g., DcR1 and DcR2) that are coexpressed on the same cell (5). Moreover, many carbohydrate-binding proteins (e.g., lectins), which demonstrate weak glycan-binding affinities ($K_D$ = mM to μM) can self-associate, increasing their avidity up to several orders of magnitude (6). The soluble, S-type lectin galectin-1 noncovalently assembles into a homodimer that can form lattices with various cell-surface glycoproteins, such as T cell receptors (TCRs) and growth factor receptors, thereby regulating different receptor signaling thresholds (7). Thus, in addition to avidity effects, lectin–glycan promiscuity is critical for modulating signal transduction.

Unlike other galectins, galectin-3 (Gal3) is the only known monomeric protein of its class to assemble into higher-ordered oligomers. The structure of a Gal3 subunit consists of an intrinsically disordered N-terminal domain (NTD) linked to a carbohydrate-recognition domain (CRD), which displays weak binding affinity and high specificity for β-galactosides (8). Biologically active Gal3 is often depicted as pentameric based on early solution-phase binding studies (9); however, in light of more recent models, other functional oligomeric states may exist due to the dynamic self-association of the NTD (10–12). While it is generally accepted that Gal3 oligomerization gives rise to avidity effects associated with its diverse functions (e.g., cell signaling and cell–cell/cell–matrix adhesion) (8), chemical strategies or tools to probe structure–function relationships for Gal3 are lacking. Other protein assemblies (e.g., antibodies) for which binding properties are established through protein–protein interactions can have drastically altered affinity, specificity, and function with as little as a single point mutation (13). In contrast, conferring selectivity toward glycans by engineering lectin–carbohydrate contact points is nontrivial and impractical (14, 15), largely because glycan sites on proteins and lipids are highly conserved.

Fascinatingly, some biological systems have evolved to overcome carbohydrate specificity through spatial rearrangement of glycans. For instance, HIV type 1 (HIV-1) hijacks host-soluble galectin-1 to facilitate gp120-CD4 interactions on $CD4^+$ T cells while glycan clustering shields gp120 from Gal3 (16). Ligand clustering

## Significance

**The family of carbohydrate-binding proteins known as galectins receive considerable attention for their ability to modulate cell behavior in both normal and pathological settings. Galectin-3, for instance, can crosslink membrane glycans to initiate, amplify, attenuate, or inhibit signal transduction pathways that lead to cell differentiation, proliferation, or death. However, understanding structure–function relationships of galectin-3 is challenged by its promiscuous glycan-binding properties and assembly into oligomers with undefined number of subunits or "valency." Here, we address these challenges by providing a toolbox of synthetic galectin-3 oligomers with tunable valency. Cell-based studies with these oligomers suggest a role for physical size as a structural determinant of galectin-3 signaling function, in addition to the increased binding strength typically associated with multivalency.**

Author contributions: S.A.F. and G.A.H. designed research; S.A.F., R.L., M.W.B., and E.A.P. performed research; S.A.F., R.L., M.W.B., E.A.P., and G.A.H. analyzed data; and S.A.F. and G.A.H. wrote the paper.

Competing interest statement: G.A.H. is a co-founder and has a financial interest in Anchor Biologics, Inc. Patents have been applied for by the University of Florida that list S.A.F. and G.A.H. as inventors.

This article is a PNAS Direct Submission.



[1]To whom correspondence may be addressed. Email: ghudalla@bme.ufl.edu.

This article contains supporting information online at https://www.pnas.org/lookup/suppl/doi:10.1073/pnas.2024117118/-/DCSupplemental.

Published May 3, 2021.

phenomena that elicit biological outputs have been recapitulated to some extent through exploration of antigen multimerization, spatial arrangement, and copy number on polymers and virus-like nanoparticles (17–19). Such synthetic approaches demonstrate that the functional role of multivalency in biology can be understood through sophisticated, bioinspired tools. Therefore, one can envision that designing multivalent Gal3 constructs via a bioinspired approach may also reveal unidentified mechanisms underpinning its structure–function relationships.

Probing multivalent lectin–glycan interactions with precise control of ligand valency and density has become possible through the development of various biologic and synthetic scaffolds (20–26). For example, we constructed a trimeric Gal3 assembly using a three-stranded α-helical coiled-coil scaffold that was previously designed by site-specific mutation of the GCN4 leucine zipper (i.e., GCN4-pM3) (27, 28). Recent work by others has demonstrated a range of synthetic coiled-coils that can self-assemble with up to 6 identical strands (29–31), presenting an opportunity for us to build an extended library of Gal3 oligomers. Here, we report synthetic Gal3 oligomers with tunable subunit valency, as well as several key discoveries that were made while using them as tools to understand emergent Gal3 function in the context of signal transduction. Synthetic oligomers were constructed through recombinant fusion of Gal3 to 2 to 6 stranded, α-helical coiled-coil scaffolds (Fig. 1 *A* and *B*). Relationships between Gal3 valency and extracellular signaling potency were established by measuring the extent to which synthetic oligomers induced death of Jurkat T cells. We identified that Gal3 signals cell death, albeit weakly, at a minimum valency of 2. We determined that CD45 regulates clustering of synthetic Gal3 oligomers. Extent of cell death via wild-type Gal3 and synthetic Gal3 oligomers decreased in the absence of CD45 or CD7. However, high valency synthetic Gal3 constructs transduced intracellular signaling cascades through pathways that altered cell fate and function in a manner that differed from wild-type Gal3, which we determined by investigating the role of caspases, interleukin-2 secretion, and pannexin-1 opening. These studies provide insight into the emergent properties of multivalent Gal3, including the influences that valency, quaternary size, and binding promiscuity have on glycan-mediated signal transduction.

## Results

**Production of Synthetic Gal3 Oligomers with Tunable Valency.** In previous work, a recombinant fusion protein was constructed by adding a flexible peptide linker between the NTD of Gal3 and the C terminus of superfolder green fluorescent protein (sfGFP), and then a trimeric assembly of the fusion protein was developed by swapping the flexible peptide linker with a peptide that noncovalently assembles into a parallel, 3-stranded α-helical coiled-coil (27, 28). In the current work, we modified the design of the trimeric assembly to construct other synthetic Gal3 oligomers by replacing the peptide linker that forms a 3-stranded coiled-coil with peptide linkers that form 2-, 4-, 5-, and 6-stranded α-helical coiled-coils (27, 29–31) (Fig. 1*A* and *SI Appendix*, Fig. S1). This approach expands our library of synthetic Gal3 constructs (i.e., Monomer, Dimer, Trimer, Tetramer, Pentamer, and Hexamer) and offers precise tunability of valency, size, and geometry for synthetic oligomerization of Gal3 (Fig. 1 *B* and *C*).

Size-exclusion chromatography (SEC) traces of synthetic Gal3 oligomers showed that proteins elute at volume fractions corresponding to their predicted native molecular weight (Fig. 1*D*). Dynamic light scattering (DLS) analysis of synthetic oligomers under native conditions further demonstrated that their hydrodynamic size scaled with predicted valency and oligomers were largely uniform at less than 20 nm in diameter (Fig. 1*E*). Empirical denatured molecular weights of the proteins, determined via gel electrophoresis, were consistent with their predicted denatured molecular weights (*SI Appendix*, Fig. S2*A*). A summary of numerical data for physical characterization studies is reported in *SI Appendix*, Table S1. Additionally, sfGFP fluorescence activity and protein concentration measured after passing oligomers through a 0.2 μm syringe filter did not significantly change, suggesting a low tendency for nonspecific protein aggregation (*SI Appendix*, Figs. S3 and S4). Taken together, these data demonstrate that the fusion proteins were successfully designed to assemble into prescribed architectures with between 2 and 6 Gal3 domains.

**Glycan-Binding Analysis of Synthetic Gal3 Oligomers.** Homomeric assembly of sfGFP-Gal3 fusion proteins leads to an equivalent valency and molar concentration of sfGFP and Gal3 within each oligomeric construct. For all experiments, the molar concentration of each construct was adjusted to ensure that the Gal3 and sfGFP concentration were held constant. A summary of the relationship between valency and molar concentration of protein constructs is shown in Fig. 2*A*.

Observed and functional affinity of multivalent ligands are coupled with ligand-receptor stoichiometry as well as the different mechanisms underlying their complexation (e.g., chelation, statistical rebinding, ligand-induced receptor clustering) (21). For multivalent Gal3, the "cluster glycoside effect" is a central mechanism of complexation and strengthens avidity interactions with glycans (32), whereas monomeric Gal3 binds to soluble carbohydrates (e.g., lactose and *N*-acetyllactosamine [LacNAc]) with relatively weak affinity ($K_D$ = mM − μM) (10). Previously, we showed that multivalent avidity effects can endow trimeric assemblies of Gal3 with higher apparent carbohydrate-binding affinity than monovalent fusion proteins using various immobilized glycan-binding assays (28). Consistent with these reports, synthetic Gal3 oligomers demonstrated a greater extent of binding to the immobilized glycoprotein asialofetuin (ASF) at saturation than the Monomer (*SI Appendix*, Fig. S5). Additionally, the half-maximal inhibitory concentration ($IC_{50}$) of LacNAc required for competitive inhibition of oligomer:ASF binding scaled with Gal3 valency (*SI Appendix*, Fig. S6).

Next, we compared the binding of wild-type Gal3 and synthetic Gal3 oligomers to immobilized lactose using α-lactose-agarose affinity chromatography. Monomer and synthetic Gal3 oligomers bound to the column and were eluted by introducing soluble β-lactose. Compared to Monomer and wild-type Gal3, which had similar elution profiles, synthetic Gal3 oligomers eluted from the column with broader profiles that shifted toward higher soluble β-lactose concentrations with increasing Gal3 valency (Fig. 2*B* and *SI Appendix*, Fig. S7). This method, which eliminates artifacts arising from measuring bound protein via sfGFP fluorescence by instead measuring absorbance (λ = 280 nm), suggests that apparent binding affinity scales with Gal3 valency.

Finally, we relied on the sfGFP domain incorporated into the fusion constructs to characterize the binding of synthetic Gal3 oligomers to membrane glycans present on the surface of Jurkat T cells. Micrographs qualitatively demonstrated that the fluorescence intensity on the cell surface increased with subunit valency of synthetic Gal3 oligomers (Fig. 2*C*). When cells with bound synthetic Gal3 oligomers were washed with 100 mM soluble β-lactose, the fluorescence signal decreased according to Gal3 valency, suggesting specific, valency-dependent binding to membrane glycans (Fig. 2*D*).

To further probe the cell-binding strength of synthetic Gal3 oligomers, we assessed the relationship between total fluorescence signal and the fluorescence signal normalized by valency. Synthetic Gal3 oligomers may demonstrate statistical rebinding, an increased probability of association, and chelate effects, where multiple receptors bind to multiple subunits of a multivalent ligand, which would increase their apparent binding affinity for membrane glycans. However, not all available Gal3 subunits are

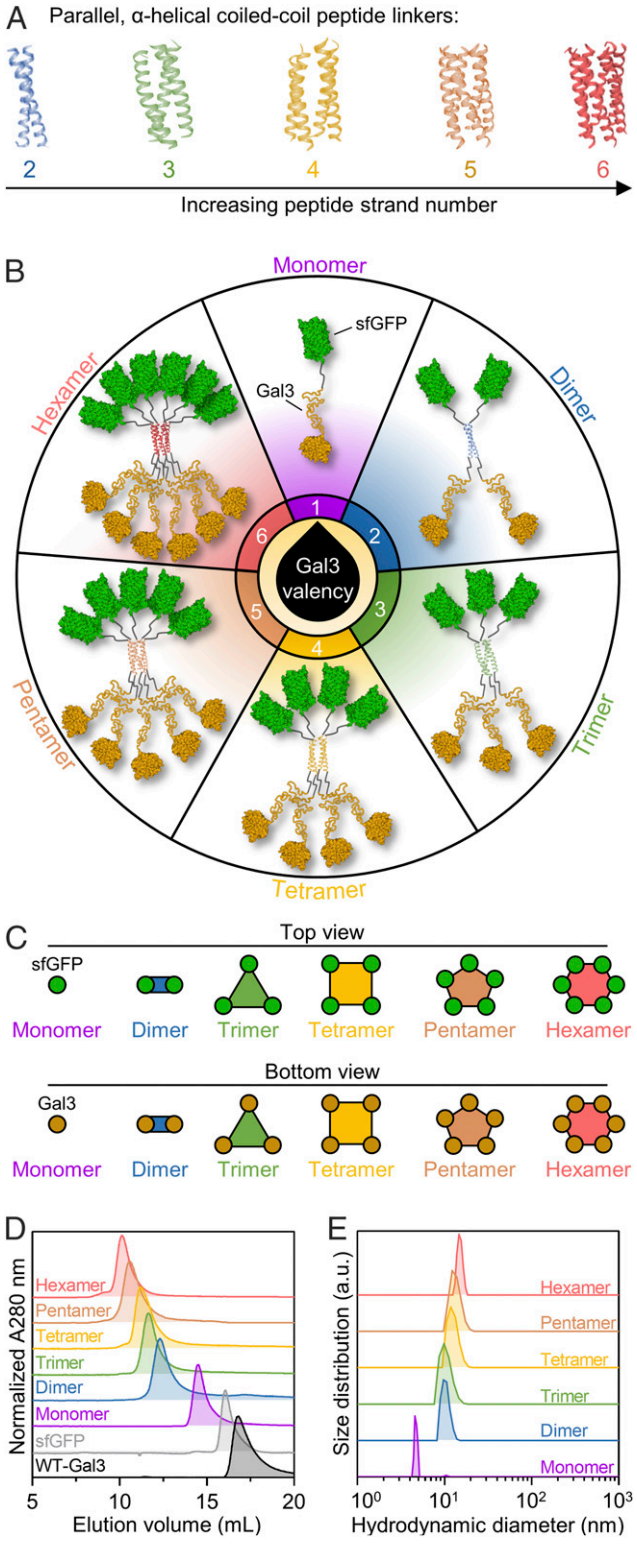


**Fig. 1.** Design and physical characterization of synthetic Gal3 constructs with tunable valency. (*A*) Library of 2- to 6-stranded parallel, α-helical coiled-coil peptide scaffolds for the assembly of defined oligomers from monomeric Gal3 fusion proteins (i.e., Monomer). (*B*) Schematic presentation of Monomer and synthetic Gal3 oligomers (i.e., Dimer-Hexamer). (*C*) Schematic presentation of Monomer-Hexamer top and bottom views. (*D*) Distribution of hydrodynamic size demonstrated via SEC. (*E*) Average hydrodynamic diameter determined via DLS. For *E*, histograms are a single representative experiment from three replicate size measurements per construct. Protein Data Bank (PDB) ID: 4DMD (2-stranded coiled-coil); 2O7H (3-stranded coiled-coil); 1GCL (4-stranded coiled-coil); 4PN8 (5-stranded coiled-coil); 3R3K (6-stranded coiled-coil); 2B3P (sfGFP); 5NF7 (Gal3 carbohydrate-recognition domain).

necessarily engaged simultaneously, which could introduce artifacts when the "output" (here, sfGFP fluorescence) is directly tied to Gal3 valency. In particular, for synthetic Gal3 oligomers, the binding of any number of Gal3 subunits to a membrane glycan, whether just one or the maximum number of subunits per construct, will localize all copies of sfGFP to the cell surface. For example, after PBS wash or soluble β-lactose wash, the total fluorescence signal of cells with bound Monomer was significantly lower than that of cells with bound synthetic Gal3 oligomers, while the bound oligomer signal generally increased with Gal3 valency (Fig. 2 *E* and *F*). However, when the total fluorescence signal after PBS wash was normalized to Gal3 valency, the bound oligomer signal was still greater than that of bound Monomer, but the signal for bound Dimer and Trimer was greater than that for Tetramer, Pentamer, and Hexamer (Fig. 2*G*). This suggested that a valency greater than 2 does not increase the extent of binding onto membrane glycans. This decrease in extent of binding with increasing valency may result from lower concentrations (i.e., mass action) of Tetramer, Pentamer, or Hexamer constructs relative to the Trimer and Dimer constructs or their larger size, which may restrict access to membrane glycans. However, when the total fluorescence signal after competitive soluble β-lactose wash was normalized to Gal3 valency, the magnitude of fluorescence signal generally scaled with Gal3 valency, demonstrating that more Gal3 remained bound even when a saturating concentration of soluble β-lactose was introduced (Fig. 2*H*). This suggested that the strength of binding between synthetic Gal3 oligomers and membrane glycans scaled with Gal3 valency, likely due to increases in effective concentration of Gal3 subunits at the cell surface which also increases with synthetic Gal3 oligomer valency.

**Characterization of the Cell Agglutination and Death Signaling Activities of Synthetic Gal3 Oligomers.** Wild-type Gal3 is known to induce clumping of cells or "agglutination" (33); however, whether agglutination is required for Gal3 to mediate proapoptotic signaling remains unknown. Under a brightfield microscope, there were no signs of Jurkat T cell agglutination following treatment with synthetic Gal3 oligomers or PBS control ("untreated") for 4 h and 18 h, whereas cells treated with wild-type-Gal3 were densely agglutinated at both time points (*SI Appendix*, Fig. S8 and Fig. 3*A*).

Extracellular Gal3 can initiate T cell apoptosis by crosslinking glycoprotein receptors, which depends on multivalent Gal3–glycan lattice formation (7, 34). Presently, and to the best of our knowledge, no studies, other than those demonstrating that Gal3 is inactive as a monomer, have shown a direct relationship between valency and apoptotic signaling. Given this unique opportunity, we first characterized the activity of synthetic Gal3 oligomers to induce cell death relative to wild-type Gal3 using the standard markers of annexin V for phosphatidylserine exposure, often linked to early apoptosis, and LIVE/DEAD for membrane permeability, which combined with phosphatidylserine exposure is often associated with late apoptosis. At both 4 h and 18 h, the extent of total cell death including both (annexin $V^+$ and LIVE/$DEAD^-$) and (annexin $V^+$ and LIVE/$DEAD^+$) cells increased with Gal3 valency, such that Hexamer induced a greater extent of cell death than wild-type Gal3 (*SI Appendix*, Fig. S9*A* and Fig. 3*B*). Notably, Gal3 in the dimeric configuration signaled cell death to a greater extent than Monomer, which was inactive as a signaling molecule, relative to the untreated control (PBS-treated cells) (Fig. 3*B*).

Next, we examined the distribution of cells into "early apoptotic" (i.e., annexin $V^+$ and LIVE/$DEAD^-$) and "late apoptotic"

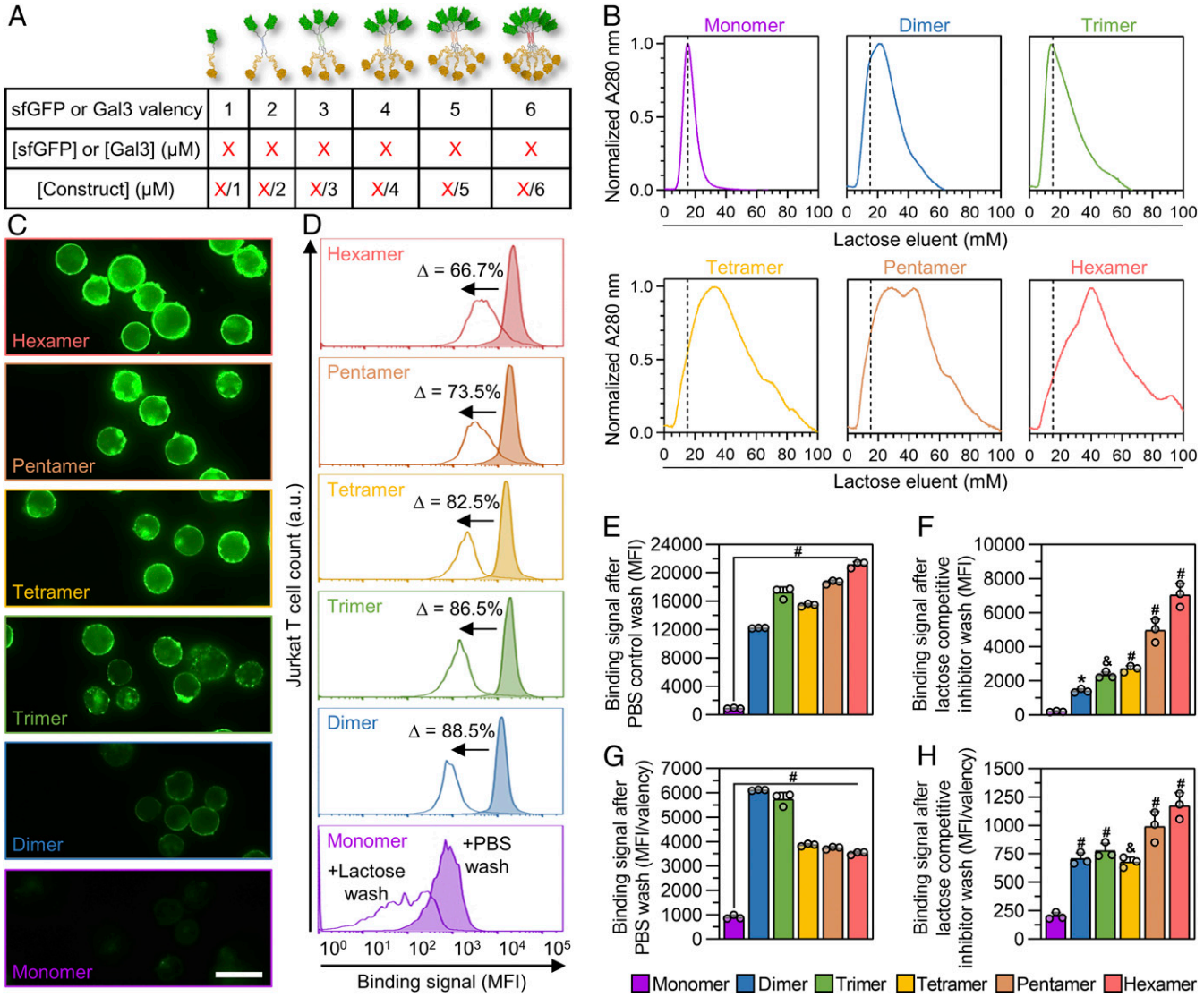


**Fig. 2.** Characterization of multivalent Gal3–glycan interactions. (*A*) Summary of the relationship between construct sfGFP/Gal3 valency, molar concentration of sfGFP/Gal3 per construct, and construct molar concentration. (*B*) Lactose affinity chromatography traces of synthetic Gal3 constructs. For comparison between monovalent and multivalent binding to α-lactose in the stationary phase, dashed lines are shown to indicate elution volume of Monomer at maximum A280 signal. (*C*) Epifluorescence microscopic images demonstrating sfGFP fluorescence output of synthetic Gal3 constructs bound to Jurkat T cells. (*D*) Competitive inhibition of synthetic Gal3 construct binding to Jurkat T cells by soluble β-lactose and PBS (negative control), as analyzed by flow cytometry. Percentages shown represent change in mean fluorescence intensity (MFI) of cell-bound synthetic Gal3 constructs after competitive inhibition with 100 mM soluble β-lactose. (*E*) Raw binding signal of cell-bound synthetic Gal3 constructs after PBS wash. (*F*) Raw binding signal of cell-bound synthetic Gal3 constructs after 100 mM soluble β-lactose wash. (*G*) Binding signal of cell-bound synthetic Gal3 constructs after PBS wash normalized to sfGFP valency of constructs. (*H*) Binding signal of cell-bound synthetic Gal3 constructs after 100 mM soluble β-lactose wash normalized to sfGFP valency of constructs. For *D*, histograms are a single representative experiment from three replicate measurements per construct and percentages shown are an average of replicates. For *E* through *H*, statistical comparisons are relative to Monomer, $n = 3$, mean ± SD, $^{*}P < 0.05$, $^{\&}P < 0.001$, $^{\#}P < 0.0001$, and comparisons were made using one-way ANOVA with Tukey's post hoc. All experiments were performed at an equimolar concentration of sfGFP or Gal3 = 5 μM (i.e., [Monomer] = 5 μM, [Dimer] = 2.5 μM, [Trimer] = 1.67 μM, [Tetramer] = 1.25 μM, [Pentamer] = 1 μM, [Hexamer] = 0.83 μM).

(i.e., annexin $V^+$ and LIVE/$DEAD^+$) populations after treatment with synthetic Gal3 oligomers and wild-type Gal3. Apart from Dimer, wild-type Gal3 and synthetic Gal3 oligomers primarily induced the early apoptotic phenotype in Jurkat T cells at 4 h (*SI Appendix*, Fig. S9*B*). At 18 h, Jurkat T cells treated with wild-type Gal3 were predominantly in the late apoptotic population, while Monomer failed to induce either early or late apoptosis, which was shown relative to the untreated control (PBS-treated cells) (Fig. 3*C*). Similar to wild-type Gal3, cells treated with Dimer, Trimer, and Tetramer were predominantly in the late apoptotic population at 18 h (Fig. 3*C*). In contrast, cells treated with Hexamer and Pentamer were more evenly distributed between the two populations at 18 h (Fig. 3*C*). Collectively, these data demonstrated that Dimer is the minimum functional Gal3 construct that can signal cell death, that the potency of cell death signaling scales with Gal3 valency, and that a synthetic construct with six Gal3 subunits, which exceeds the historically assumed active Gal3 valency by one subunit, can signal more cell death than the wild-type protein. However, differences between the distribution of cells into early and late apoptotic populations following treatment with wild-type Gal3 versus Pentamer and Hexamer suggested that these synthetic Gal3 oligomers may signal cell death through pathways that differ from that of wild-type Gal3.

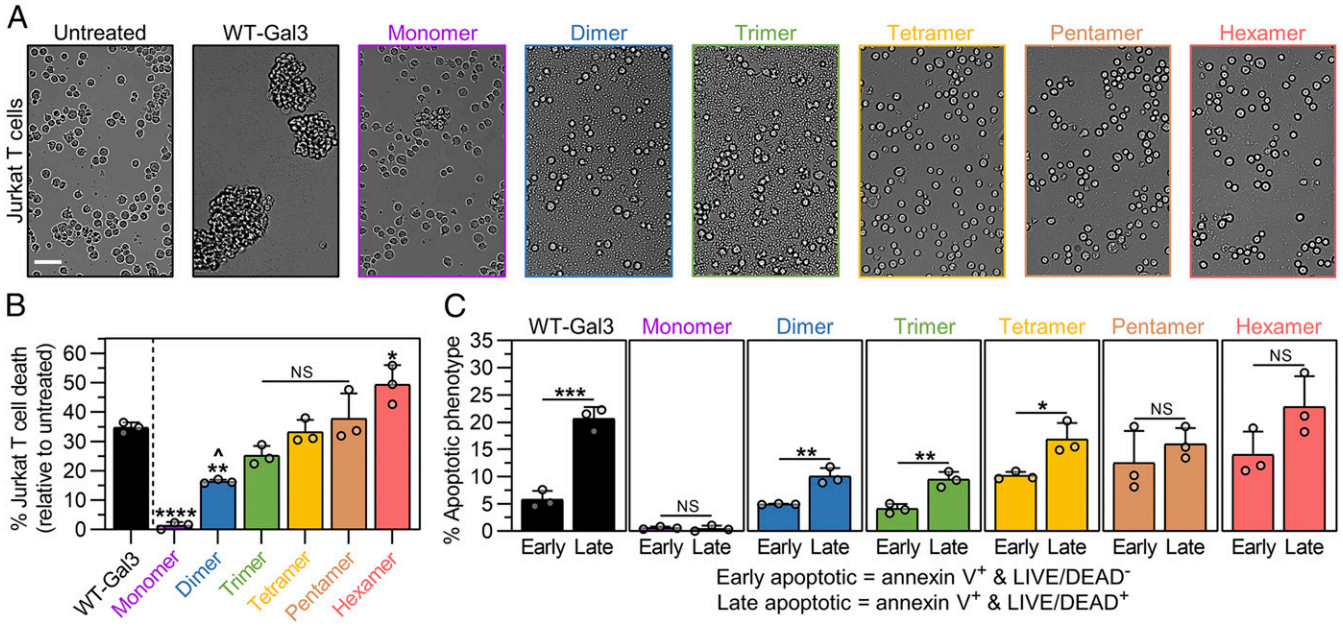


**Fig. 3.** Cell agglutination and death signaling activities of synthetic Gal3 constructs. (*A*) Brightfield microscopic images taken of Jurkat T cells after 18 h incubation with synthetic Gal3 constructs, wild-type Gal3 (WT-Gal3), or PBS (untreated control). (Scale bar, 50 μm.) (*B*) Percentage of Jurkat T cell death after 18 h treatment with synthetic Gal3 constructs or WT-Gal3, shown relative to the untreated control. (*C*) Percentage of Jurkat T cells in the early apoptotic and late apoptotic populations after 18 h treatment with synthetic Gal3 constructs or WT-Gal3, shown relative to the untreated control. For *B*, $n = 3$, mean ± SD, $*/\text{^}P < 0.05$, $**P < 0.01$, $****P < 0.0001$, NS is no significant difference, and comparisons were made using one-way ANOVA with Tukey's post hoc. Statistical comparisons relative to WT-Gal3 are denoted by * or NS symbol. Statistical comparison relative to Monomer is denoted by ^ symbol. For *C*, $n = 3$, mean ± SD, $*P < 0.05$, $**P < 0.01$, $***P < 0.001$, NS is no significant difference, and comparisons were made using unpaired two-tailed Student's *t* test. All experiments were performed at an equimolar concentration of sfGFP or Gal3 = 5 μM (i.e., [WT-Gal3] = 5 μM, [Monomer] = 5 μM, [Dimer] = 2.5 μM, [Trimer] = 1.67 μM, [Tetramer] = 1.25 μM, [Pentamer] = 1 μM, [Hexamer] = 0.83 μM).

**Membrane Glycan Clustering and Cell Death Signaling Activities of Synthetic Gal3 Oligomers Are Regulated by CD45.** Extracellular wild-type Gal3 can differentially engage and crosslink various membrane glycoprotein receptors (e.g., CD7, CD29, CD45, CD71) to trigger T cell death (35, 36). It is valuable to understand the biological mechanisms and outcomes of these promiscuous Gal3-receptor interactions for pharmaceutical applications or drug discovery (e.g., design of selective Gal3 inhibitors or biomimetic Gal3 agonists). In addition to the Jurkat T cell line, two different receptor-deficient lymphocyte cell lines, J45.01 ($CD45^-/CD7^+$) and HuT 78 ($CD45^+/CD7^-$), have been used previously to characterize the role of CD45 and CD7 in wild-type Gal3-mediated membrane glycan clustering and cell death signaling (36, 37). Unlike J45.01 and HuT 78 T cells, Jurkat T cells express both CD45 and CD7, which differ both in size and availability on the cell surface (Fig. 4*A*). The observed differences in extent of Jurkat T cell death, as well as the distribution of cells into early and late apoptotic populations (Fig. 3 *B* and *C*), prompted us to study the roles of CD45 and CD7 in cell binding, glycan clustering, and death signaling activity of the synthetic Gal3 oligomers relative to wild-type Gal3.

Hexamer bound to both J45.01 and HuT 78 T cells, albeit to a lesser extent on the former after a PBS wash (*SI Appendix*, Fig. S10). After a 100 mM soluble β-lactose wash, more Hexamer remained bound to J45.01 T cells than on HuT 78 T cells. Specifically, there was an 81.3% decrease in binding signal of Hexamer on J45.01 T cells, and a 92.9% decrease in binding signal of Hexamer on HuT 78 T cells after the soluble β-lactose wash (*SI Appendix*, Fig. S10). Relative to the 66.7% decrease in binding signal of Hexamer on Jurkat T cells after a 100 mM soluble β-lactose wash (Fig. 2*C*), these data suggested that the presence of both CD45 and CD7 increases the strength of Hexamer binding to the cell surface and that Hexamer remains more tightly bound to cells lacking CD45 than CD7.

Confocal microscopic images of Hexamer-treated Jurkat, J45.01, and HuT 78 T cells stained via anti-CD45 and anti-CD7 immunofluorescence show that the types of membrane glycoproteins that are present influence the distribution of Hexamer on the cell surface. As expected, CD45 signal was low on J45.01 T cells, while CD7 signal was low on HuT 78 T cells relative to Jurkat T cells (Fig. 4*B* and *SI Appendix*, Figs. S11 and S12). Hexamer was uniformly distributed on Jurkat T cells and HuT 78 T cells but was found in large, polarized clusters on J45.01 T cells (Fig. 4*B* and *SI Appendix*, Figs. S11 and S12). This clustering may explain, in part, the tighter binding of Hexamer to J45.01 T cells relative to HuT 78 T cells. The distribution of Hexamer on Jurkat T cells and HuT 78 T cells generally correlated with the distribution of CD45 on these cells (Fig. 4*B* and *SI Appendix*, Figs. S11 and S12). In contrast, the clustered and polarized distribution of Hexamer on J45.01 T cells did not appear to colocalize with CD7, which was uniformly distributed on Jurkat T cells but predominantly outside of the sfGFP-rich clusters on J45.01 T cells (Fig. 4*C* and *SI Appendix*, Figs. S11 and S12). These observations suggested that membrane glycoconjugates other than CD7 are involved in Hexamer clustering when CD45 is absent from the cell surface and that when CD45 is present, Hexamer remains evenly distributed in a pattern that is consistent with the distribution of CD45.

Wild-type Gal3 induced agglutination of J45.01 and HuT 78 T cells, whereas Pentamer and Hexamer did not, similar to the agglutination activity of each protein with Jurkat T cells (*SI Appendix*, Fig. S13). This suggested that CD45 and CD7 are not involved in agglutination or that their absence can be compensated for by other membrane glycoconjugates.

Hexamer, Pentamer, and wild-type Gal3 induced the death of both J45.01 T cells and HuT 78 T cells; however, the extent of cell death induced by each protein was significantly diminished when either CD45 or CD7 was absent. In particular, relative to

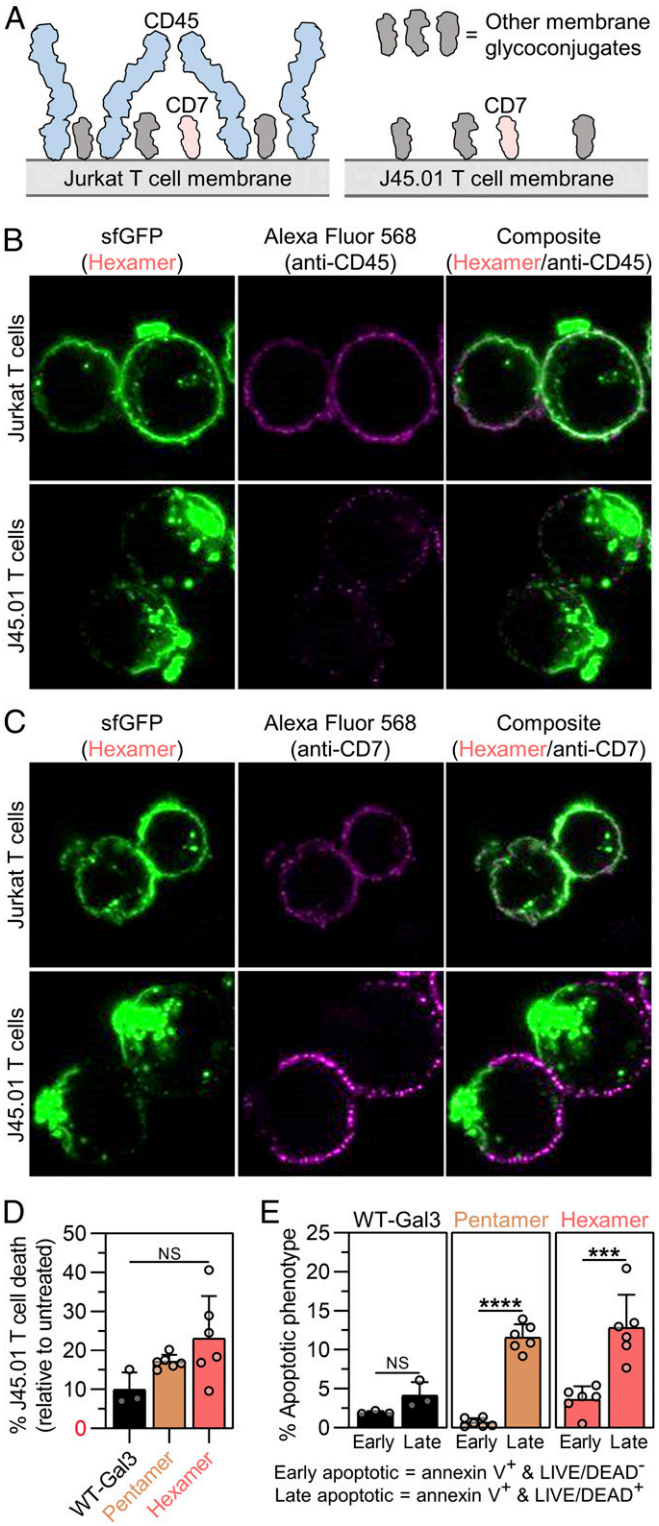


**Fig. 4.** CD45 regulates membrane glycan clustering and cell death signaling activity of synthetic Gal3 oligomers. (*A*) Schematic presentation of membrane glycoconjugates that Gal3 can engage on Jurkat and J45.01 T cells. Membrane glycoprotein CD45 is distinguished from other membrane glycoconjugates, such as CD7, by its relatively larger size. Jurkat T cells are $CD45^+$ and $CD7^+$, whereas J45.01 T cells are $CD45^-$ and $CD7^+$. (*B*) Confocal microscopic images of Hexamer (green) and CD45 (magenta) following Hexamer treatment of Jurkat T cells and J45.01 T cells for 2 h. (*C*) Confocal microscopic images of Hexamer (green) and CD7 (magenta) following Hexamer treatment of Jurkat T cells and J45.01 T cells for 2 h. (*D*) Percentage of J45.01 T cell death after 18 h treatment with synthetic Gal3 oligomers or wild-type Gal3 (WT-Gal3), shown relative to the PBS-treated cells (untreated control). (*E*) Percentage of J45.01 T cells in the early apoptotic or late apoptotic population after 18 h treatment with synthetic Gal3 oligomers or WT-Gal3, shown relative to the untreated control. For *D*, $n \geq 3$, mean ± SD, NS is no significant difference, and comparisons were made using one-way ANOVA with Tukey's post hoc. For *E*, $n \geq 3$, mean ± SD, $^{***}P < 0.001$, $^{****}P < 0.0001$, NS is no significant difference, and comparisons were made using unpaired two-tailed Student's *t* test. All experiments were performed at an equimolar concentration of sfGFP or Gal3 = 5 μM (i.e., [WT-Gal3] = 5 μM, [Pentamer] = 1 μM, [Hexamer] = 0.83 μM).

Jurkat T cells, Hexamer induced ~53% less J45.01 T cell death and ~72% less HuT 78 T cell death; Pentamer induced ~55% less J45.01 T cell death and ~46% less HuT 78 T cell death; and wild-type Gal3 induced ~71% less J45.01 T cell death and ~82% less HuT 78 T cell death (Fig. 4*D* and *SI Appendix*, Fig. S14*A*). Collectively, these observations demonstrated that wild-type Gal3 and synthetic Gal3 oligomers depend on both CD45 and CD7 to signal cell death, although loss of either glycoprotein has a more pronounced effect on wild-type Gal3 activity than that of either Pentamer or Hexamer. Further, loss of CD7 had a greater effect on Hexamer activity than Pentamer activity.

J45.01 T cells treated with wild-type Gal3 were more evenly distributed between early and late apoptotic populations, whereas J45.01 T cells treated with Pentamer and Hexamer were predominantly in the late apoptotic population (Fig. 4*E*). In contrast, HuT 78 T cells treated with wild-type Gal3 were mostly in the early apoptotic population, whereas cells treated with synthetic Gal3 oligomers were more evenly distributed between the populations (*SI Appendix*, Fig. S14*B*). Notably, the distribution of HuT 78 T cells treated with Pentamer and Hexamer was similar to that of Jurkat T cells treated with these constructs (Fig. 3*C*), whereas the distribution of J45.01 T cells treated with these constructs was significantly different. This suggested that CD45 may occlude Pentamer and Hexamer engagement of membrane glycans located beneath CD45, which is abundant and extends far from the cell surface (Fig. 4*A*), due to the large size of these synthetic oligomers relative to wild-type Gal3 in the unassembled state. Further, these data suggested that CD7 is necessary for wild-type Gal3 to signal the transition from early to late apoptosis, whereas its role in signaling via Pentamer and Hexamer is not obvious.

**CD45 Regulates the Caspase Dependence of Apoptotic Signaling via Synthetic Gal3 Oligomers and Wild-Type Gal3.** Promiscuous binding, such as that observed between wild-type Gal3 and membrane glycans, makes it difficult to discern the relationship between the receptors that are engaged during outside-in signaling and their involvement in activating or inhibiting particular intracellular signaling pathways. For example, apoptosis induced by extracellular wild-type Gal3 has been suggested to depend on CD45 but not CD43, whereas conflicting roles of CD7 and CD29 are reported (35, 36). Early reports suggested that extracellular wild-type Gal3 signals apoptosis through cytochrome *c*-release and caspase-3 activation independent of caspase-8 activation (35), whereas more recent reports suggested that wild-type Gal3 activates caspase-9 and caspase-3 through phosphorylation of extracellular signal-regulated kinase (38). Prior reports have also shown that antibody-mediated crosslinking of CD45 can induce caspase-independent cell death (39). Having now identified CD45 as a key mediator of Gal3 signaling and a regulator of Hexamer clustering, we next studied the role of caspases in cell death signaling via wild-type Gal3, Pentamer, and Hexamer in the presence and absence of CD45. Synthetic Gal3 oligomers and wild-type Gal3 induced less Jurkat T cell death when cells were pretreated with a pan-caspase inhibitor (Fig. 5*A*). Synthetic Gal3 oligomers and wild-type Gal3 also induced less J45.01 T cell death with pancaspase

inhibition (Fig. 5*B*). A plot of the effectiveness of the pancaspase inhibitor, represented as the percent change in apoptosis between its presence and absence, suggested that wild-type Gal3 apoptosis signaling in Jurkat T cells had a stronger caspase-dependence than Pentamer, while Hexamer had an intermediate dependence on caspases (Fig. 5 *C*, *Left*). In J45.01 T cells, which lack CD45, the pancaspase inhibitor was significantly more effective at inhibiting apoptosis via wild-type Gal3, Pentamer, and Hexamer than in Jurkat T cells, although Pentamer and Hexamer could still signal some apoptosis, whereas wild-type Gal3 could not (i.e., 100% inhibition of apoptosis) (Fig. 5 *C*, *Right*). Collectively, these data suggest that CD45 regulates the apoptosis signaling pathway that is activated by wild-type Gal3 and synthetic Gal3 oligomers and that its presence leads to a diminished role for caspases. Notably, the ability of CD45 to diminish the role of caspases in apoptotic signaling is more pronounced for synthetic Gal3 oligomers than wild-type Gal3, which may reflect the large size or static quaternary architecture of the former. Further, these data suggest that caspase activation via Hexamer correlates with its tendency to cluster on the cell surface, which is enabled by the absence of CD45.

**Synthetic Gal3 Oligomers Induce Cell Death with Diminished IL-2 Secretion due to the Lack of Caspase-Mediated Pannexin-1 Hemichannel Opening.** The observation that Pentamer and Hexamer induced greater cell death with a weaker caspase-dependence than wild-type Gal3 led to the assumption that other caspase-dependent cell activities are possibly altered as well. For instance, wild-type Gal3 stimulates Jurkat T cells to secrete the cytokine interleukin (IL)-2 (40). Earlier reports have shown that caspase-mediated opening of the plasma membrane hemichannel pannexin-1 in early apoptotic T cells can allow for selective conduction of adenosine triphosphate (ATP) and fluorescent dyes (e.g., TO-PRO-3) across the plasma membrane (41, 42), and other studies indicate that extracellular ATP released via pannexin-1 can stimulate IL-2 secretion in an autocrine fashion (43, 44); however, in late apoptosis, this selectivity for fluorescent dye transport is lost due to increased membrane permeability (Fig. 6*A*). Our studies demonstrate that Pentamer and Hexamer induced significantly less IL-2 secretion from Jurkat T cells than cells treated with wild-type Gal3 (Fig. 6*B*). Hexamer also induced significantly less activation of the initiator caspase, caspase-8, in Jurkat T cells than cells treated with wild-type Gal3 (*SI Appendix*, Fig. S15). Likewise, Hexamer induced less activation of effector caspases, caspase-3/-7, in Jurkat T cells than cells treated with wild-type Gal3, whereas Pentamer induced even less caspase-3/-7 activation than Hexamer (Fig. 6*C*). Collectively, these data correlated with the observations in Fig. 5, which suggested that Pentamer and Hexamer signal cell death through a pathway that is less dependent on caspases than wild-type Gal3.

Informed by these observations, we then studied the opening of pannexin-1 via wild-type Gal3 and Hexamer using an established selective TO-PRO-3 uptake experiment (Fig. 6*A*) (41, 42). As a positive control, Jurkat T cells treated with anti-Fas antibody, a potent apoptogenic ligand with high specificity for the Fas death receptor, induced rapid and selective TO-PRO-3 uptake in a caspase- and pannexin-1-dependent manner (*SI Appendix*, Fig. S16). Cells treated with wild-type Gal3 also exhibited significant TO-PRO-3 uptake in a pannexin-1- and caspase-dependent fashion, albeit with less potency and slower kinetics than the anti-Fas positive control (8 h versus 4 h to maximum uptake, respectively) (Fig. 6*D*). By 12 h and 18 h, uptake of TO-PRO-3 by cells treated with wild-type Gal3 was no longer dependent on pannexin-1 but did depend on caspases, which suggested that these cells exhibited greater membrane permeability as they entered later stages of apoptosis. Recall that Jurkat T cells treated with wild-type Gal3 were also permeable to the pannexin-1-impermeable dye LIVE/DEAD at 18 h when they were predominantly in the late apoptotic population (Fig. 3*C*). In contrast, low-level uptake of TO-PRO-3 by Jurkat T cells treated with Hexamer at 4 h and 8 h did not depend on caspase activation or pannexin-1 opening. Similar to wild-type Gal3 treatment, increased TO-PRO-3 uptake in Jurkat T cells treated with Hexamer at 12 h and 18 h did not depend on pannexin-1 but did depend on caspases, albeit to a lesser extent than wild-type Gal3. This was consistent with observations that apoptosis induced by synthetic Gal3 oligomers was less dependent on caspases than apoptosis induced by wild-type Gal3 (Fig. 4). Collectively, these results suggest that

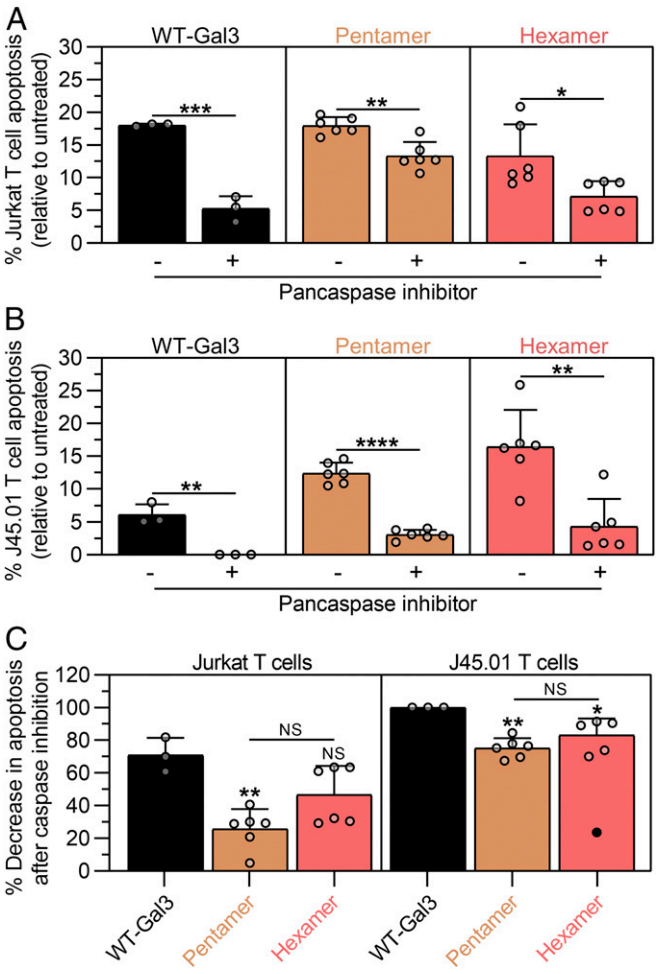


**Fig. 5.** CD45 governs the dependence on caspases for cell death signaling via wild-type Gal3, Pentamer, and Hexamer. (*A*) Percentage of Jurkat T cell apoptosis after 18 h treatment with synthetic Gal3 oligomers or wild-type Gal3 (WT-Gal3) relative to PBS-treated cells (untreated) while in the presence or absence of a pancaspase inhibitor. (*B*) Percentage of J45.01 T cell apoptosis after 18 h treatment with synthetic Gal3 oligomers or WT-Gal3 relative to untreated cells while in the presence or absence of a pancaspase inhibitor. (*C*) Percentage decrease in Jurkat and J45.01 T cell apoptosis after caspase inhibition from data in *A* and *B*. For *A* and *B*, $n \geq 3$, mean ± SD, $^{*}P < 0.05$, $^{**}P < 0.01$, $^{***}P < 0.001$, $^{****}P < 0.0001$, NS is no significant difference, and comparisons were made using unpaired two-tailed Student's *t* test. For *C*, $n \geq 3$, mean ± SD, $^{*}P < 0.05$, $^{**}P < 0.01$, NS is no significant difference, and comparisons were made using one-way ANOVA with Tukey's post hoc. Statistical comparisons relative to WT-Gal3-treated Jurkat or J45.01 T cells are denoted by * or NS symbol directly above bars, and one outlier (black circle) was detected using Grubbs' test while removed from mean ± SD calculation. All experiments were performed at an equimolar concentration of sfGFP or Gal3 = 5 μM (i.e., [WT-Gal3] = 5 μM, [Pentamer] = 1 μM, [Hexamer] = 0.83 μM).

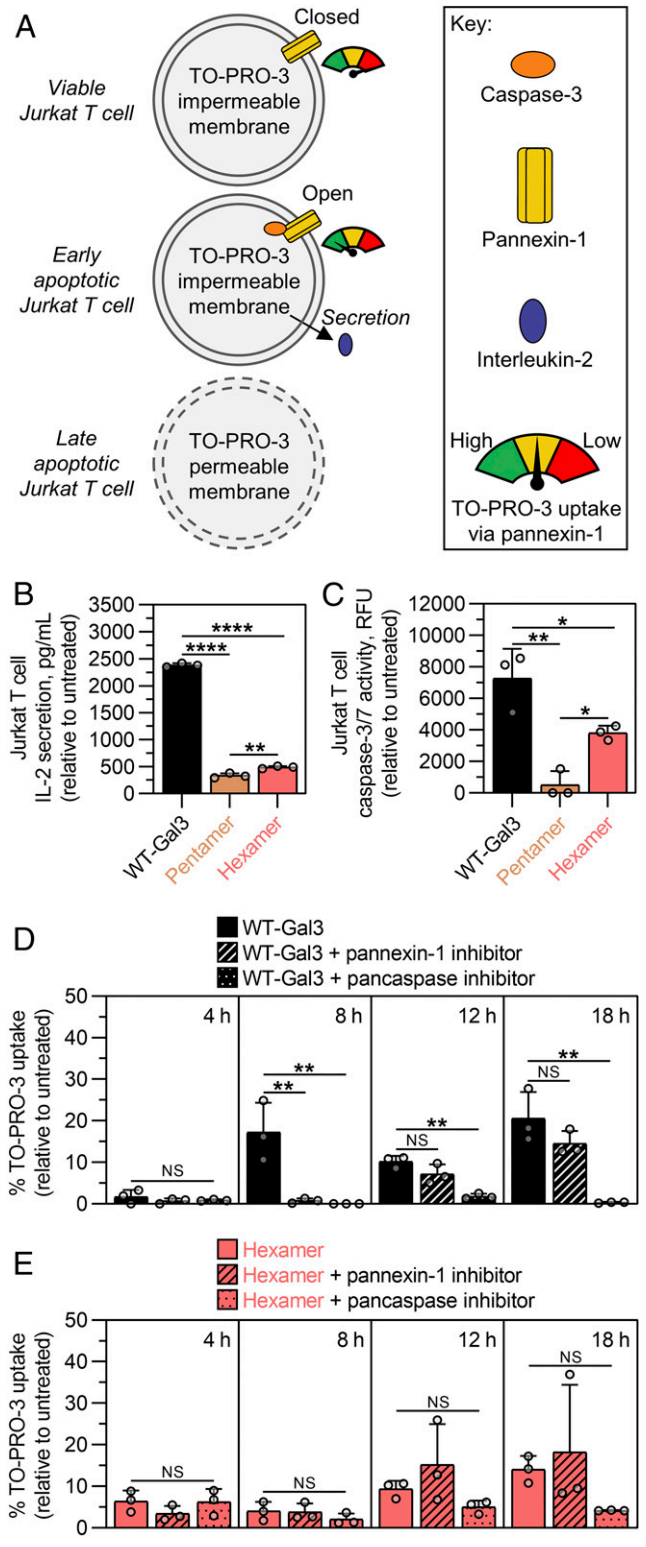


**Fig. 6.** Synthetic Gal3 oligomers induce Jurkat T cell death with diminished IL-2 secretion due to the lack of caspase-mediated pannexin-1 hemichannel opening. (*A*) Schematic presentation of caspase-mediated Jurkat T cell apoptosis and opening of plasma membrane hemichannel pannexin-1, which can selectively conduct adenosine triphosphate outward to stimulate IL-2 secretion in a purinergic receptor-mediated autocrine fashion. Extent of pannexin-1 opening is measured by the amount of selective uptake of the membrane-impermeable dye, TO-PRO-3. However, as apoptosis progresses into later stages, the cell membrane becomes more permeable to TO-PRO-3. (*B*) Concentration of IL-2 secreted from Jurkat T cells following 18 h treatment with synthetic Gal3 oligomers or wild-type Gal3 (WT-Gal3), shown relative to the PBS-treated cells (untreated control). (*C*) Caspase-3/-7 activity of Jurkat T cells following 18 h treatment with synthetic Gal3 oligomers or WT-Gal3, shown relative to the untreated control. (*D*) Percentage of TO-PRO-3 uptake by Jurkat T cells following different treatment times with WT-Gal3 in the presence and absence of a pannexin-1 inhibitor or pancaspase inhibitor. (*E*) Percentage of TO-PRO-3 uptake by Jurkat T cells following different treatment times with Hexamer in the presence and absence of a pannexin-1 inhibitor or pancaspase inhibitor. For *B* through *E*, $n = 3$, mean ± SD, $^{*}P < 0.05$, $^{**}P < 0.01$, $^{****}P < 0.0001$, NS is no significant difference, and comparisons were made using one-way ANOVA with Tukey's post hoc. All experiments were performed at an equimolar concentration of sfGFP or Gal3 = 5 μM (i.e., [WT-Gal3] = 5 μM, [Pentamer] = 1 μM, [Hexamer] = 0.83 μM).

synthetic Gal3 oligomers induce considerably less caspase-mediated opening of pannexin-1 than wild-type Gal3, which results in diminished secretion of IL-2 by cells treated with the former.

## Discussion

Here, we created a library of well-defined synthetic Gal3 oligomers as tools to study valency-function relationships, such as Gal3 binding to cell membrane glycans and activation of outside-in signal transduction. Understanding multivalent galectin–glycan interactions is important for designing therapeutic galectin inhibitors and recapitulating galectin effector function. For instance, galectin-1 can act as an extracellular signaling molecule that downregulates inflammation and adaptive immune responses by crosslinking glycoprotein receptors involved in T cell death via reversible assembly into a homodimer (36, 45, 46). Delivery of wild-type galectin-1 to suppress or reverse T cell-dependent immunopathologies has long represented a promising therapeutic strategy (47); however, its poor stability in physiological conditions limits its biological activity in preclinical settings (48). In recent years galectin-1 has been engineered to form stable dimers with increased activity using polymer- and peptide-based scaffolds (47, 49). Wild-type Gal3, on the other hand, undergoes dynamic assembly into oligomers with ill-defined valency, which represents a major challenge for probing its emergent biological functions in physiological and pathological conditions. The library of coiled-coil scaffolds implemented in this work was critical for constructing a tunable set of stable Gal3 oligomers with precisely controlled subunit valency. This approach allowed us to generate a range of oligomers informed by the suggested natural valency of wild-type Gal3. We show that the cell-binding properties of synthetic Gal3 oligomers scales with the number of Gal3 subunits. Potency to signal T cell death also scales with the number of Gal3 subunits. However, the signaling pathways that are activated by synthetic oligomers differ from the pathway activated by wild-type Gal3, leading to differences in downstream responses, such as opening of the pannexin-1 hemichannel and secretion of IL-2. Collectively, these studies identified important relationships between valency, avidity, and the dynamic nature of wild-type Gal3 oligomerization in the context of its promiscuous binding and emergent extracellular signaling activity.

The observation that synthetic Gal3 oligomers can signal apoptosis without inducing agglutination (Fig. 3) suggested that they can engage with membrane glycans in *cis* (on one cell) but not in *trans* (between 2 or more cells), which contrasts starkly with wild-type Gal3 that can engage in both *cis* and *trans*. The absence of agglutination among cells treated with synthetic Gal3 oligomers that undergo apoptosis demonstrates that these two events are not operatively linked. Notably, wild-type Gal3 induces agglutination of cells that express CD45 and CD7, as well as cells that are deficient in either receptor, suggesting that these membrane glycoproteins are either not involved in agglutination

or can be compensated for by other membrane glycans. It is unclear exactly how the structure of Gal3 enables its engagement with glycoproteins in *cis* or *trans*. Compared to galectin-1, which has been proposed to form crystalline lattices due to its homodimeric structure, Gal3 has been proposed to form amorphous lattices due its tendency to form higher-ordered oligomers (50). Recent models suggest that Gal3 can engage with glycoproteins in *trans* due to liquid–liquid phase separation of its intrinsically disordered NTD, which results in the formation of an amorphous supramolecular structure (12). Early models suggested that galectins engage a single type of glycoprotein to form lattices (51). Consistent with this, we previously reported that a synthetic heterodimer of galectin-1 linked to Gal3 cannot induce agglutination or signal apoptosis, likely because galectin-1 and Gal3 signal death through different receptors; however, a synthetic heterotetramer with two galectin-1 and two Gal3 domains on opposing termini of a coiled-coil could induce agglutination and signal apoptosis (49). It is well known that galectin-1 is active as a homodimer, which supports the observed function of the heterotetramer, whereas the minimal functional oligomer of Gal3 was unknown. Here, we showed that the minimum valency for Gal3 activity is also 2, consistent with a report showing that both galectin-1 and Gal3 contribute to the signaling activity of the heterotetramer (37). In contrast to the heterotetramer design, here the Gal3 domains were fused to one terminus of a parallel, α-helical coiled-coil while sfGFP was fused to the other. This Janus-like design seems to bias Gal3 to engage in *cis* irrespective of the valency of the Gal3 domain. It remains to be determined if sfGFP sterically impedes the engagement of synthetic Gal3 oligomers in *trans* or if the restricted mobility of Gal3 domains tethered to a coiled-coil is the molecular feature that prevents *trans* interactions. Along these lines, fusion of a protein (e.g., sfGFP) onto the N terminus of Gal3 knocks out its ability to induce agglutination and apoptosis, without compromising monovalent carbohydrate binding, demonstrating that an appended cargo can disrupt natural oligomerization of Gal3 via its NTD.

The data presented here demonstrate that CD45 regulates Hexamer clustering and signaling pathway activation, likely by governing membrane glycoprotein recognition, and that CD45 has differing effects on synthetic Gal3 oligomer signaling activity relative to that of wild-type Gal3 (Figs. 4–6). Wild-type Gal3 is thought to be incapable of forming higher-ordered oligomers in the absence of multivalent glycan binding (9) and is therefore thought to exist largely in the monomeric form in the solution. We postulate that monomeric wild-type Gal3 can engage glycans closer to the cell surface, such as CD7, more effectively than high valency synthetic oligomers because it can more efficiently traffic through the dense population of membrane glycans that are present on the T cell surface. There are two physical features that inform this thinking. First, the wild-type Gal3 monomer, which is smaller than the fusion Monomer reported here, is considerably smaller than either Pentamer or Hexamer (Fig. 2), which will enable more rapid and efficient transport through a dense environment. Second, monovalent Gal3-glycan interactions are weak and labile (10), exemplified here by Monomer (Fig. 2), which leads to rapid dissociation of wild-type Gal3 from any membrane glycan it binds to in the absence of a local Gal3 concentration that is sufficient to nucleate oligomer formation. In contrast, the avidity effects that arise from synthetically fixing Gal3 oligomerization via fusion to an α-helical coiled-coil (Fig. 2) lead to increases in apparent binding affinity with the most probable partner Gal3 will encounter. It is reasonable that this partner would be the glycosylated molecules that are most abundant and most accessible on the cell surface, which for T cells is CD45. Indeed, confocal microscopy images showed that the distribution of Hexamer on the surface of Jurkat T cells correlated with the distribution of CD45 (Fig. 4). However, the data presented here also show that both CD45 and CD7 are essential for cell death signaling via both wild-type Gal3 and synthetic Gal3 oligomers (Fig. 4 and *SI Appendix*, Fig. S14). Confocal images suggest that Hexamer clusters in the absence of CD45 with membrane glycans other than those found on CD7; however, the absence of CD7 decreased cell death signaling via Hexamer, Pentamer, and wild-type Gal3, with a much greater effect on Hexamer and wild-type Gal3 than Pentamer. We propose that CD45 may facilitate interactions between Gal3 and CD7 to activate caspase-dependent cell death signaling. Considering existing models that propose that homotypic receptor crosslinking is favored for prototype and chimeric galectins (51), heterotypic crosslinking involving both CD45 and CD7 working in concert would support a model in which valency greater than 2 is the functional state of Gal3. Consistent with this, we observed that Dimer can signal cell death, with an early/late apoptotic cell distribution that was similar to that of Hexamer treated cells lacking CD45, albeit with much lower potency. Notably, we see more caspase activation with Hexamer than with Pentamer, and Hexamer has a stronger dependence on caspase activation to signal death than Pentamer. This may suggest that the increased valency of Hexamer allows it to concurrently engage CD45 and CD7, in addition to other presently unidentified membrane glycans, more effectively than Pentamer, leading to an increased role for caspases as mediators of cell death signaling.

Collectively, the data reported here demonstrate that engineering galectin-binding specificity for a particular glycoprotein receptor remains a significant challenge. Introducing site-specific mutations within the carbohydrate-binding pocket and adjacent binding sites of Gal3 can confer fine specificity for soluble carbohydrates (52). Here, we found that synthetically fixing Gal3 oligomerization can overcome some of its glycan-binding promiscuity, leading to some tunability of the intracellular signaling pathways that are activated. Thus, although selective recognition has not yet been realized, coupling the use of α-helical coiled-coils as multivalent scaffolds with other protein engineering strategies may one day enable such precision.

In conclusion, we presented a synthetic strategy to tune Gal3 valency using a library of 2- to 6-stranded α-helical coiled-coil scaffolds. Synthetic Gal3 oligomers provided a set of probes to investigate relationships between valency and emergent Gal3 function. With these probes, we identified the minimum valency of Gal3 required to signal cell death. We also established a modality to physically tune promiscuous Gal3 signaling, exemplified through CD45-dependent changes to the dependence of caspases and the preference of oligomers to signal in *cis* but not *trans*, which may be more broadly applicable to lectins and other multivalent signaling proteins. Hexamer demonstrated greater potency to signal T cell death than wild-type Gal3, with weaker IL-2 release, highlighting the potential of synthetic Gal3 oligomers as immunomodulatory drugs. We envision this scaffolding platform will be invaluable for probing mechanisms of Gal3-glycan interactions, as well as guiding the development of therapeutics that modulate Gal3 signaling.

## Materials and Methods

The materials and methods are described in detail in *SI Appendix*. Recombinant protein constructs were cloned and expressed in Origami B(DE3) Competent Cells and then purified using immobilized metal affinity chromatography and SEC on an ÄKTA pure system. Protein size was analyzed via gel electrophoresis, SEC, and DLS. Reporter protein activity was measured via spectrophotometry. Glycan binding assays were performed through α-lactose-agarose affinity chromatography on an ÄKTA pure system as well as saturation and competitive binding assays on microplates accompanied by spectrophotometric analysis of bound reporter protein activity. Cell binding measurements and images were collected using flow cytometry and epifluorescence microscopy, respectively. Cell death was determined by annexin V and LIVE/DEAD staining, and caspase-dependence of cell death signaling was evaluated in the presence and absence of a pan-caspase inhibitor. Cell agglutination assays were performed in microplates, and then images of cells were taken via brightfield microscopy. Confocal

images of membrane glycoproteins were taken after cells were treated with Hexamer, then bound by primary monoclonal antibodies selective for either CD45 or CD7, and finally stained with Alexa Fluor 568-conjugated secondary Immunoglobulin G (IgG) antibody. Caspase activity and IL-2 secretion was quantified using instructions from commercially available assay kits. Cell uptake of TO-PRO-3 was measured in the presence of either a pancaspase inhibitor or pannexin-1 inhibitor using flow cytometry. Statistical analyses are reported in figure legends as well as in *SI Appendix*. Schematics were drawn using Illustrate (53).

**Data Availability.** All study data are included in the article and/or *SI Appendix*.

**ACKNOWLEDGMENTS.** This work was supported by the NIH (National Institute of Biomedical Imaging and Bioengineering, 5-R03-EB019684-02; National Institute of Dental and Craniofacial Research, 1-R01-DE027301-01) and in part by the NIH/National Center for Advancing Translational Sciences Clinical and Translational Science Awards to the University of Florida UL1TR001427 and TL1TR001428. Work in the E.A.P. laboratory is supported by the NIH (National Institute of Diabetes and Digestive and Kidney Diseases, 1-F31-DK126397-01A1; 1-R01-DK124267-01A1) and JDRF (2-SRA-2019-781-S-B). The content is solely the responsibility of the authors and does not necessarily represent the official views of the NIH. We thank Dr. Carlos Rinaldi for access to his DLS instrument. We also thank Adithya Gopinath for providing advice on flow cytometry.

1. R. Pancsa, E. Schad, A. Tantos, P. Tompa, Emergent functions of proteins in non-stoichiometric supramolecular assemblies. *Biochim. Biophys. Acta. Proteins Proteomics* **1867**, 970–979 (2019).
2. P. Li *et al*., Phase transitions in the assembly of multivalent signalling proteins. *Nature* **483**, 336–340 (2012).
3. J. E. Ladbury, S. T. Arold, Noise in cellular signaling pathways: Causes and effects. *Trends Biochem. Sci.* **37**, 173–178 (2012).
4. H. L. Goel, A. M. Mercurio, VEGF targets the tumour cell. *Nat. Rev. Cancer* **13**, 871–882 (2013).
5. L. O'Leary *et al*., Decoy receptors block TRAIL sensitivity at a supracellular level: The role of stromal cells in controlling tumour TRAIL sensitivity. *Oncogene* **35**, 1261–1270 (2016).
6. R. D. Cummings, R. L. Schnaar, J. D. Esko, K. Drickamer, M. E. Taylor, "Principles of glycan recognition" in *Essentials of Glycobiology*, A. Varki., Eds. (Cold Spring Harbor Laboratory Press, Cold Spring Harbor, NY, 2017), pp. 373–385.
7. O. B. Garner, L. G. Baum, Galectin-glycan lattices regulate cell-surface glycoprotein organization and signalling. *Biochem. Soc. Trans.* **36**, 1472–1477 (2008).
8. J. Dumic, S. Dabelic, M. Flögel, Galectin-3: An open-ended story. *Biochim. Biophys. Acta* **1760**, 616–635 (2006).
9. N. Ahmad *et al*., Galectin-3 precipitates as a pentamer with synthetic multivalent carbohydrates and forms heterogeneous cross-linked complexes. *J. Biol. Chem.* **279**, 10841–10847 (2004).
10. J. Seetharaman *et al*., X-ray crystal structure of the human galectin-3 carbohydrate recognition domain at 2.1-A resolution. *J. Biol. Chem.* **273**, 13047–13052 (1998).
11. Y. H. Lin *et al*., The intrinsically disordered N-terminal domain of galectin-3 dynamically mediates multisite self-association of the protein through fuzzy interactions. *J. Biol. Chem.* **292**, 17845–17856 (2017).
12. Y. P. Chiu *et al*., Liquid-liquid phase separation and extracellular multivalent interactions in the tale of galectin-3. *Nat. Commun.* **11**, 1229 (2020).
13. T. A. Whitehead *et al*., Optimization of affinity, specificity and function of designed influenza inhibitors using deep sequencing. *Nat. Biotechnol.* **30**, 543–548 (2012).
14. S. Tommasone *et al*., The challenges of glycan recognition with natural and artificial receptors. *Chem. Soc. Rev.* **48**, 5488–5505 (2019).
15. J. Hirabayashi, R. Arai, Lectin engineering: The possible and the actual. *Interface Focus* **9**, 20180068 (2019).
16. C. St-Pierre *et al*., Host-soluble galectin-1 promotes HIV-1 replication through a direct interaction with glycans of viral gp120 and host CD4. *J. Virol.* **85**, 11742–11751 (2011).
17. E. B. Puffer, J. K. Pontrello, J. J. Hollenbeck, J. A. Kink, L. L. Kiessling, Activating B cell signaling with defined multivalent ligands. *ACS Chem. Biol.* **2**, 252–262 (2007).
18. N. R. Bennett, D. B. Zwick, A. H. Courtney, L. L. Kiessling, Multivalent antigens for promoting B and T cell activation. *ACS Chem. Biol.* **10**, 1817–1824 (2015).
19. R. Veneziano *et al*., Role of nanoscale antigen organization on B-cell activation probed using DNA origami. *Nat. Nanotechnol.* **15**, 716–723 (2020).
20. M. Mammen, S. K. Choi, G. M. Whitesides, Polyvalent interactions in biological systems: Implications for design and use of multivalent ligands and inhibitors. *Angew. Chem. Int. Ed. Engl.* **37**, 2754–2794 (1998).
21. L. L. Kiessling, J. E. Gestwicki, L. E. Strong, Synthetic multivalent ligands in the exploration of cell-surface interactions. *Curr. Opin. Chem. Biol.* **4**, 696–703 (2000).
22. C. R. Bertozzi, L. L. Kiessling, Chemical glycobiology. *Science* **291**, 2357–2364 (2001).
23. A. H. Courtney, E. B. Puffer, J. K. Pontrello, Z. Q. Yang, L. L. Kiessling, Sialylated multivalent antigens engage CD22 in trans and inhibit B cell activation. *Proc. Natl. Acad. Sci. U.S.A.* **106**, 2500–2505 (2009).
24. L. L. Kiessling, J. C. Grim, Glycopolymer probes of signal transduction. *Chem. Soc. Rev.* **42**, 4476–4491 (2013).
25. A. Restuccia, Y. F. Tian, J. H. Collier, G. A. Hudalla, Self-assembled glycopeptide nanofibers as modulators of galectin-1 bioactivity. *Cell. Mol. Bioeng.* **8**, 471–487 (2015).
26. A. Restuccia *et al*., Evaluation of self-assembled glycopeptide nanofibers modified with N,N′-diacetyllactosamine for selective galectin-3 recognition and inhibition. *ACS Biomater. Sci. Eng.* **4**, 3451–3459 (2018).
27. B. Ciani *et al*., Molecular basis of coiled-coil oligomerization-state specificity. *Proc. Natl. Acad. Sci. U.S.A.* **107**, 19850–19855 (2010).
28. S. A. Farhadi *et al*., Locally anchoring enzymes to tissues via extracellular glycan recognition. *Nat. Commun.* **9**, 4943 (2018).
29. P. B. Harbury, T. Zhang, P. S. Kim, T. Alber, A switch between two-, three-, and four-stranded coiled coils in GCN4 leucine zipper mutants. *Science* **262**, 1401–1407 (1993).
30. N. R. Zaccai *et al*., A de novo peptide hexamer with a mutable channel. *Nat. Chem. Biol.* **7**, 935–941 (2011).
31. A. R. Thomson *et al*., Computational design of water-soluble α-helical barrels. *Science* **346**, 485–488 (2014).
32. J. J. Lundquist, E. J. Toone, The cluster glycoside effect. *Chem. Rev.* **102**, 555–578 (2002).
33. J. Xue *et al*., Regulation of galectin-3-induced apoptosis of Jurkat cells by both O-glycans and N-glycans on CD45. *FEBS Lett.* **587**, 3986–3994 (2013).
34. I. R. Nabi, J. Shankar, J. W. Dennis, The galectin lattice at a glance. *J. Cell Sci.* **128**, 2213–2219 (2015).
35. T. Fukumori *et al*., CD29 and CD7 mediate galectin-3-induced type II T-cell apoptosis. *Cancer Res.* **63**, 8302–8311 (2003).
36. B. N. Stillman *et al*., Galectin-3 and galectin-1 bind distinct cell surface glycoprotein receptors to induce T cell death. *J. Immunol.* **176**, 778–789 (2006).
37. S. A. Farhadi, M. M. Fettis, R. Liu, G. A. Hudalla, A synthetic tetramer of galectin-1 and galectin-3 amplifies pro-apoptotic signaling by integrating the activity of both galectins. *Front Chem.* **7**, 898 (2020).
38. H. Xue *et al*., The N-terminal tail coordinates with carbohydrate recognition domain to mediate galectin-3 induced apoptosis in T cells. *Oncotarget* **8**, 49824–49838 (2017).
39. S. Lesage *et al*., CD4+ CD8+ thymocytes are preferentially induced to die following CD45 cross-linking, through a novel apoptotic pathway. *J. Immunol.* **159**, 4762–4771 (1997).
40. D. K. Hsu, S. R. Hammes, I. Kuwabara, W. C. Greene, F. T. Liu, Human T lymphotropic virus-I infection of human T lymphocytes induces expression of the beta-galactoside-binding lectin, galectin-3. *Am. J. Pathol.* **148**, 1661–1670 (1996).
41. F. B. Chekeni *et al*., Pannexin 1 channels mediate 'find-me' signal release and membrane permeability during apoptosis. *Nature* **467**, 863–867 (2010).
42. I. K. Poon *et al*., Unexpected link between an antibiotic, pannexin channels and apoptosis. *Nature* **507**, 329–334 (2014).
43. U. Schenk *et al*., Purinergic control of T cell activation by ATP released through pannexin-1 hemichannels. *Sci. Signal.* **1**, ra6 (2008).
44. B. Rissiek, F. Haag, O. Boyer, F. Koch-Nolte, S. Adriouch, P2X7 on mouse T cells: One channel, many functions. *Front. Immunol.* **6**, 204 (2015).
45. N. L. Perillo, K. E. Pace, J. J. Seilhamer, L. G. Baum, Apoptosis of T cells mediated by galectin-1. *Nature* **378**, 736–739 (1995).
46. L. V. Norling, M. Perretti, D. Cooper, Endogenous galectins and the control of the host inflammatory response. *J. Endocrinol.* **201**, 169–184 (2009).
47. S. A. Farhadi, G. A. Hudalla, Engineering galectin-glycan interactions for immunotherapy and immunomodulation. *Exp. Biol. Med. (Maywood)* **241**, 1074–1083 (2016).
48. M. Cho, R. D. Cummings, Galectin-1, a β-galactoside-binding lectin in Chinese hamster ovary cells. II. Localization and biosynthesis. *J. Biol. Chem.* **270**, 5207–5212 (1995).
49. M. M. Fettis, S. A. Farhadi, G. A. Hudalla, A chimeric, multivalent assembly of galectin-1 and galectin-3 with enhanced extracellular activity. *Biomater. Sci.* **7**, 1852–1862 (2019).
50. C. F. Brewer, M. C. Miceli, L. G. Baum, Clusters, bundles, arrays and lattices: Novel mechanisms for lectin-saccharide-mediated cellular interactions. *Curr. Opin. Struct. Biol.* **12**, 616–623 (2002).
51. G. A. Rabinovich, M. A. Toscano, S. S. Jackson, G. R. Vasta, Functions of cell surface galectin-glycoprotein lattices. *Curr. Opin. Struct. Biol.* **17**, 513–520 (2007).
52. E. Salomonsson *et al*., Mutational tuning of galectin-3 specificity and biological function. *J. Biol. Chem.* **285**, 35079–35091 (2010).
53. D. S. Goodsell, L. Autin, A. J. Olson, Illustrate: Software for biomolecular illustration. *Structure* **27**, 1716–1720.e1 (2019).